Research paper

New solvent blends for post-combustion CO_2 capture

Hanna K. Knuutila*, Rune Rennemo, Arlinda F. Ciftja

Norwegian University of Science and Technology, Department of Chemical Engineering, NO-7491 Trondheim, Norway

Abstract

In the current work five different solvent blends are experimentally studied and the reboiler duties are calculated using the so-called short-cut method. Tertiary amines, 2-(diethylamino)ethanol (DEEA), 3-(Diethylamino)-1,2-propanediol (DEA-12PD), 2-[2-(Diethylamino)ethoxy] ethanol (DEA-EO), 1-(2-Hydroxyethyl)piperidine (12HE-PP) are blended with 3-(Methylamino)propylamine (MAPA) and ethanolamine (MEA). The first results from simple solvent screening are given and the cyclic capacities are calculated based data at 40 °C and 80 °C. Then, five solvent systems are chosen for vapor−liquid equilibrium characterization. The vapor−liquid equilibrium data are then used to estimate cyclic capacities at more realistic temperatures, between 40 °C and 120 °C and by using a short-cut method proposed in the literature the reboiler duties of the characterized solvents are estimated. Finally, the potential of the studied systems is discussed. Several of the characterized blends showed reboiler duties around 2.5 MJ $kg_{CO_2}^{-1}$.

1. Introduction

Fossil fuels cover around 80% of the world's energy demand at present and they will also be the main energy sources in the years to come [1]. Fossil fuel combustion and industrial processes account for about 65% of total global greenhouse gas emissions. Power production and the industrial sectors are the main emitters of CO_2. They are considered to play a major role in global warming, and represent considerable potential for decreasing CO_2 emissions by means of capture and storage. CO_2 capture can be carried out in power plants with post-combustion, oxy-fuel or pre-combustion technologies. Chemical absorption, where CO_2 is captured and released in a cyclic process is the most mature technology and has been used for decades. Typically, CO_2 is absorbed into the aqueous solvent system at temperatures between 40 °C to 65 °C and desorbed from the solution after heating. The maximum temperature in the regeneration is typically around 120 °C. The process uses often aqueous amines and the greatest heat requirement stems

from regeneration of the solvent. Thus, many research groups are working on finding solvent systems with low energy requirements during solvent regeneration.

The alkanolamines are typically divided into three main categories: primary, secondary and tertiary. Both primary and secondary amines react with CO_2 forming carbamates with overall reaction:

$$CO_2 + 2RNH_2 \leftrightarrow RNHCOO^- + RNH_3^+$$

The primary and secondary amines form a fairly stable carbamate requiring more energy to reverse the reaction compared to tertiary amines reacting with CO_2, through base catalysis of CO_2 hydration:

$$CO_2 + R_1R_2R_3 - N + H_2O \leftrightarrow R_1R_2R_3 - NH^+ + HCO_3^-$$
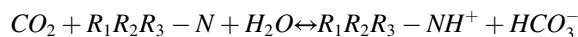
However, whereas the heat of absorption and reaction rate are high in the case of primary and secondary amines, the tertiary amines have a lower heat of absorption and a slower reaction rate [2]. Consequently, a tertiary amine or amine blend with a high absorption rate and a low heat of reaction

---

* Corresponding author.
  E-mail address: hanna.knuutila@ntnu.no (H.K. Knuutila).

could reduce the regeneration energy [2,3]. As a result, blends containing tertiary amines have been widely studied [4–6].

In the present work, tertiary amines, DEA-12PD, 12-HE-PP and DEEA are blended with MAPA or MEA. The absorption capacity, reported in the literature, at 40 °C for the amine components present in the blends in this work are shown in Fig. 1. From the figure we can see that all the single components absorb more CO_2 (mol $kg_{solvent}^{-1}$) than aqueous MEA. It seems that the three tertiary amines, 12-HE-PP, DEEA and DEA-12PD can absorb around 30% more than MEA. MAPA is able to absorb almost twice the amount of CO_2 compared to MEA. This can be explained by the structure of primary/secondary diamine (MAPA). As a multiamine, it has more functional groups available for absorption of CO_2. Fig. 2 presents the cyclic capacities reported in the literature. Although the experimental conditions vary somewhat, some trends can be seen. First, MAPA was found to have considerable ability to absorb CO_2 at as 40 °C shows a very low cyclic capacity. Secondly, DEEA seems to give the highest cyclic capacity (except at 70 °C) followed by 1(2HE)PP and DEA-1,2-PD. It seems that in all these tertiary amines the cyclic capacity is very dependent on the regeneration temperature. It should be mentioned that the partial pressure of CO_2 in the studies shown in the figure vary from 10 to 20 kPa explaining some of the scatter seen.

At the same time as Figs. 1 and 2 illustrate the potential of these solvent components, they also reveal a potential problem with fast screening experiments being able to identify good solvents. In the screening experiments to identify promising solvents, the cyclic capacity is often used as one of the main selection criteria. In the figures, the scatter is clearly visible between the equilibrium data (filled markers) and the screening experiments (open markers). In some cases the screening results show even higher loadings than that reached in the equilibrium experiments. Recently, I.M. Bernhardsen and H.K. Knuutila [7] discussed this issue and concluded that accurate liquid loading determination is crucial and that the screening experiments should not be terminated based on time limitation, rather the
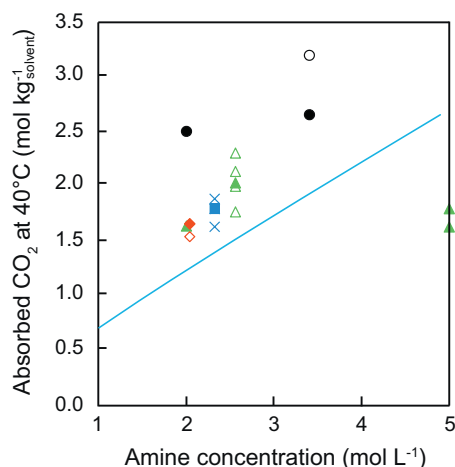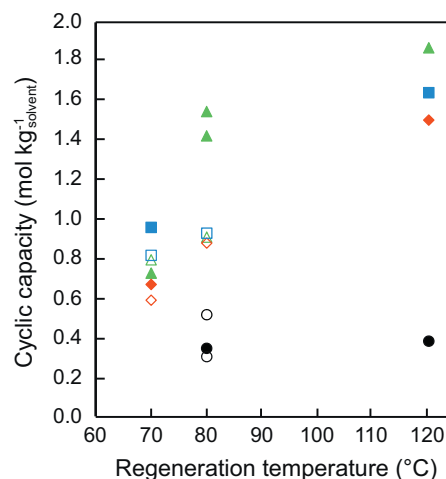

Fig. 2. Reported cyclic capacity of the single solvents 1-(2HE)PP, DEA-1,2PD, DEEA, MAPA and MEA. ●/○ MAPA from [8,9] ■/□; 1-(2HE)PP from [3,11]; ▲/△ DEEA from [3,8,10–12,12,13]; ◆/◇ DEA-1,2-PD [3,11]. Filled markers are based on the VLE data, open markers are data from the screening experiments.

partial pressure of CO_2 leaving the reactor should be used. Finally (when possible), the experiments should be performed under realistic process conditions, since the regeneration temperature has a substantial influence on the cyclic capacity.
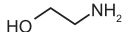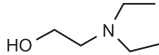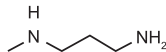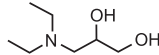
The current work has three main objectives:
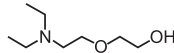
1) Report new VLE data for new solvent blends containing a tertiary amine and MEA or MAPA.
2) Calculate the reboiler duties using a short-cut method for four solvent blends and compare the characterized solvent blends with the literature data.
3) To further discuss the challenges of using cyclic capacity to identify promising solvent blends measured using screening experiments where the desorption is performed at 80 °C.

In the current work we study the potential of four tertiary amines promoted with two different primary amines. The tested tertiary amines are 2-(diethylamino)ethanol (DEEA), 3-(Diethylamino)-1,2-propanediol (DEA-12PD), 2-[2-(Diethylamino)ethoxy]ethanol (DEA-EO) and cyclic tertiary amine 1-(2-Hydroxyethyl)piperidine (12HE-PP). The promoters used are 3-(Methylamino)propylamine (MAPA) and ethanolamine (MEA). The first results from simple solvent screening are given and the cyclic capacities are calculated based on data at 40 °C and 80 °C. Then four solvent systems are chosen for vapor–liquid equilibrium (VLE) characterization. The vapor–liquid equilibrium data are then used to estimate cyclic capacities at between 40 °C and 120 °C and by using a short-cut method proposed by H. Kim, S.J. Hwang and K.S. Lee [14], the reboiler duties of the characterized solvents are estimated. Finally, the potential of the studied systems is discussed by comparing the estimated reboiler duties to other new solvent systems proposed in the literature.

1.1. Literature review

Aqueous DEEA has been screened by several authors [3,10–12] as shown in Figs. 1 and 2. In addition to the screening data,

Fig. 1. Absorbed CO_2 at 40 °C into the single solvents 1-(2HE)PP, DEA-1,2PD, DEEA, MAPA and MEA. ●/○ MAPA from [8–10]; ■/□; 1-(2HE)PP from [3,11]; ▲/△ DEEA from [3,8,10–13]; ◆/◇ DEA-1,2-PD from [3,11]. Filled markers are based on the VLE data, open markers are data from the screening experiments.

Table 1
Chemicals used in this work.

Name	Synonyms	Structure	CAS	pKa (20 °C)
Ethanolamine	MEA		141-43-5	9.5
2-(diethylamino)ethanol	DEEA; DEAE		100-37-8	9.87
3-(Methylamino)propylamine	MAPA		6291-84-5	10.5
3-(Diethylamino)-1,2-propanediol	DEA-12PD		621-56-7	9.69
1-(2-Hydroxyethyl)piperidine	12HE-PP		3040-44-6	9.57
2-[2-(Diethylamino)ethoxy]ethanol	DEA-EO		140-82-9	10.15

vapor–liquid equilibria has been reported covering unloaded and CO_2-loaded systems [8,13,15,16]. Based on the data several VLE models have also been published [13,17,18]. These papers provide more detailed literature reviews of the available data as well as models and will not be repeated here. In addition to the VLE data, experimental data on the heat of absorption of DEEA has been measured by [4,19]. They found that the heat of absorption of CO_2 was below 60 kJ $mol_{CO_2}^{-1}$ at 40 °C. For aqueous DEEA, kinetic data are also available [20–23] and an extensive literature review can be found in [24].

Two investigators [9,10] carried out a screening of aqueous MAPA whereas [8,25] provided both experimental VLE data as well as an equilibrium model for aqueous MAPA. Arshad et al. and Kim & Svendsen [4,19] reported the heat of absorption of CO_2 for aqueous MAPA to be between 80 and 90 kJ $mol_{CO_2}^{-1}$, which was much higher compared to aqueous DEEA (tertiary amine) [19]. Finally, [26] measured the absorption rates in unloaded solutions of aqueous MAPA over a large concentration range.

Both 12-HE-PP and DEA-12PD were tested in a screening setup [3,11] as also shown in Figs. 1 and 2. Surplus to the screening data, one source of kinetic data was found [27]. No heat of absorption or VLE data was found.

There are some data available for the blends of DEEA with other amines. The most studied is DEEA + MAPA blends, where the focus has mainly been on solvent blends forming two liquid phases [4,8,18,28]. Lately, [29] studied the effect of MAPA concentration on the heat of absorption for one phase systems containing DEEA and MAPA and [21] measured the absorption kinetics. There have also been other studies testing the potential of DEEA promoted with MEA, PZ and EEA [30–33]. Brœder and Svendsen [32] tested the absorption capacity of DEEA + MEA at 40 °C and concluded that MEA was not a good promoter for DEEA and that both Piperazine (Pz) and MAPA increased the absorption capacity at 40 °C more than MEA. Another study on DEEA + MEA reported cyclic capacities

around 0.14–0.2 mol_{CO_2} mol_{amine}^{-1} or 0.84–1.26 mol_{CO_2} L^{-1} when calculated between 40 °C and 100 °C [33]. In the current work, we do not test the DEEA promoted with MEA, rather we compare our results with the literature data [33]. Data for MEA or MAPA blended with 12-HEPP and DEA-12PD were not found.

The following conclusions can be drawn from the literature review: firstly, the potential of 12-HE-PP and DEA-12PD as a potential tertiary amine in MAPA or MEA promoted blends has not been previously studied. Furthermore, even though several studies with DEEA + MAPA blends have been published, in most of the studies the focus has been on solutions that form two liquid phases under CO_2 absorption.

2. Experimental work

2.1. Chemicals

In this work MEA ($\geq$ 99.5%, SIGMA), DEEA ($\geq$ 99.5%, SIGMA), MAPA ($\geq$ 97%, SIGMA), DEA-12PD ($\geq$ 98%, TCI), DEA-EO ($\geq$ 98%, TCI) and 12HE-PP ($\geq$ 98%, TCI) were used without further purification. The structures and CAS numbers are given in Table 1. In addition, N_2 (99.6%) and CO_2 (99.999%) from AGA Gas GmbH were used. The Table 1 shows that the tertiary amines chosen have dissociation constant values, pKa, higher than MEA. The pKa value of an amine solvent is important since the reaction rate increases with pKa [34,35]. Furthermore, G. Puxty, R. Rowland, A. Allport, Q. Yang, M. Bown, R. Burns, M. Maeder and M. Attalla [10] showed that the absorption capacity of tertiary amines was strongly correlated with pKa. All solutions were prepared at room temperature using DI-water.

2.2. Screening

A screening apparatus, shown in Fig. 3 was used during the screening experiments [36–40]. The apparatus gives a fast
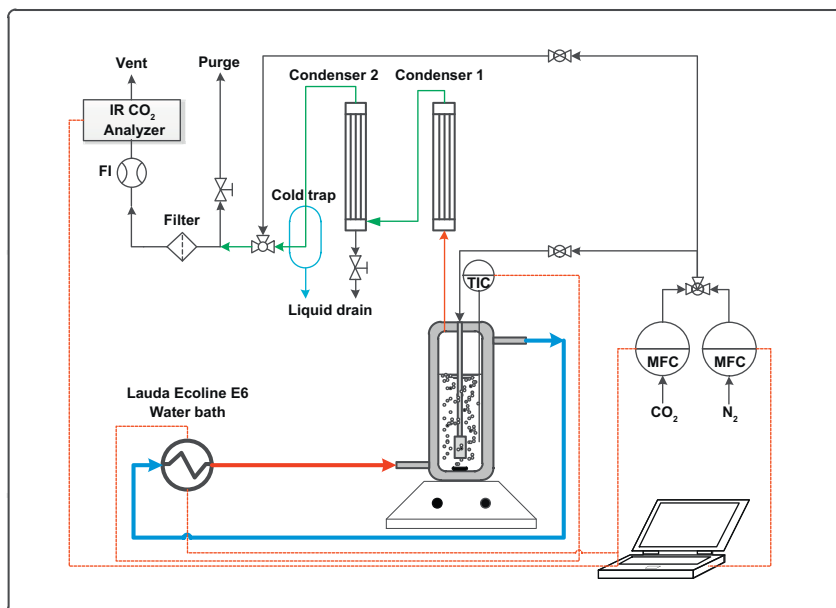
Fig. 3. Screening Apparatus [11] (MFC = Mass Flow Controller; TIC = Temperature Indicator and Controlled); FI = Flow Indicator (Rotameter); IR = Infrared).

estimation of the solvent performance, by first measuring the absorption capacity at 40 °C under relevant CO_2 partial pressures and then measuring how easily the system strips CO_2 at 80 °C. In the experiments, a $\sim 200\ cm^3$ jacketed glass reactor was filled with known amount of solution (~120 g) and stirred with a magnetic stirrer to improve the gas liquid contact. The liquid temperature in the reactor (uncertainty ± 0.1 °C) was controlled by a Lauda Ecoline E6 water bath. During the absorption process, the temperature was 40 °C. Two Bronkhors® High-Tech mass flow controllers (MFC), one for N_2 (0–5 NL min^{-1}) and one for CO_2 (0–1 NL min^{-1}), were used to provide 1NL min^{-1} gas flow with 10 vol% CO_2 into the reactor. The gas leaving the reactor was cooled down with jacketed double-coil condensers. Condensate from the first condenser was returned into the reactor. Any carry-over condensate was collected in a separation funnel after the second condenser. After that the gas stream was sent through a cold trap and a gas filter before the gas entered the Fisher–Rosemount BINOS® 100 NDIR CO_2 analyzer measuring the CO_2 content in the exit gas. When the gas outlet concentration showed 9.5%, the absorption was finished. Then a liquid sample was withdrawn and the solution temperature was increased to 80 °C. When the solution temperature reached 80 °C, nitrogen was bubbled through the solution, until the CO_2 analyzer showed 1.0% CO_2 and the desorption process was automatically stopped and a liquid sample was withdrawn.

With the logged data the absorption rate was calculated using this equation:

$$r_{CO_2}\left(\frac{mol\ CO_2}{kg\ solution \cdot s}\right) = \frac{1}{W_S} \cdot n_{CO_2}^{in} - \frac{x_{CO_2}^{Out} \cdot n_{N_2}^{In}}{1 - x_{CO_2}^{Out}} \qquad (1)$$

In the equation $W_S(kg)$ is the amount of solvent in the reactor, $x_{CO_2}^{Out}(-)$ is the volume (%) of CO_2 in the gas leaving the reactor, $n_{CO_2}^{in}\left(\frac{mol}{s}\right)$ and $n_{N_2}^{In}\left(\frac{mol}{s}\right)$ are the amounts of CO_2 and

N_2 fed into the reactor, respectively. The cyclic capacity was calculated as the difference between the lean and rich loadings determined by the liquid analyses.

2.3. Vapor-liquid experiments

Atmospheric pressure (low-temperature) VLE apparatus: The apparatus and experimental procedure used for equilibrium measurements at low pressure have previously been described by several authors [41–43]. Thus, only a short description of the experimental procedure is given here. The apparatus shown in Fig. 4 is designed to operate at temperatures up to 80 °C and consists of four 360 cm³ glass flasks, an X-STREAM CO_2 Gas Analyzer (XEGK) equipped with 2 channels for CO_2 (0–1 ± 0.1% and 0–100 ± 0.5%), a BÜHLER pump (Type 2), and two K-type thermocouples (±0.1 °C) measuring the temperature of the heated cabined and the solution (flask 4). 150 cm³ of the solution pre-loaded with CO_2 was fed into flasks 2, 3 and 4 while flask 1 was used as gas stabilizer. The flasks were placed in a thermostate box and were heated by water. After the solution and the cabinet reached the desired temperature, circulation of the gas phase was started. Equilibrium was obtained when the CO_2-analyzer showed a constant value and a liquid sample was withdrawn and analyzed for CO_2 content and amine concentration. The experiments were repeated for each solvent system in order to understand the overall experimental repeatability.

The partial pressure of CO_2 (p_{CO_2}) was calculated according to [37,39,44]:

$$p_{CO_2} = y_{CO_2} \bullet \left(P_{amb} - p_{Solvent}^{T_{Exp}} + p_{Solvent}^{T_{Cond}}\right) \qquad (2)$$

where y_{CO_2} is the CO_2 concentration measured by the CO_2 analyzer (vol %), P_{amb} is the ambient pressure, $p_{Solvent}^{Exp}$ is the vapor pressure of the solvent at experimental temperature and
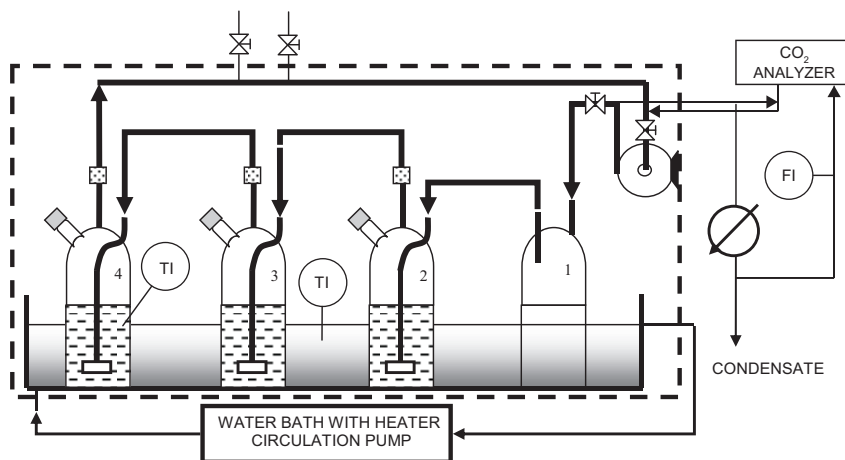
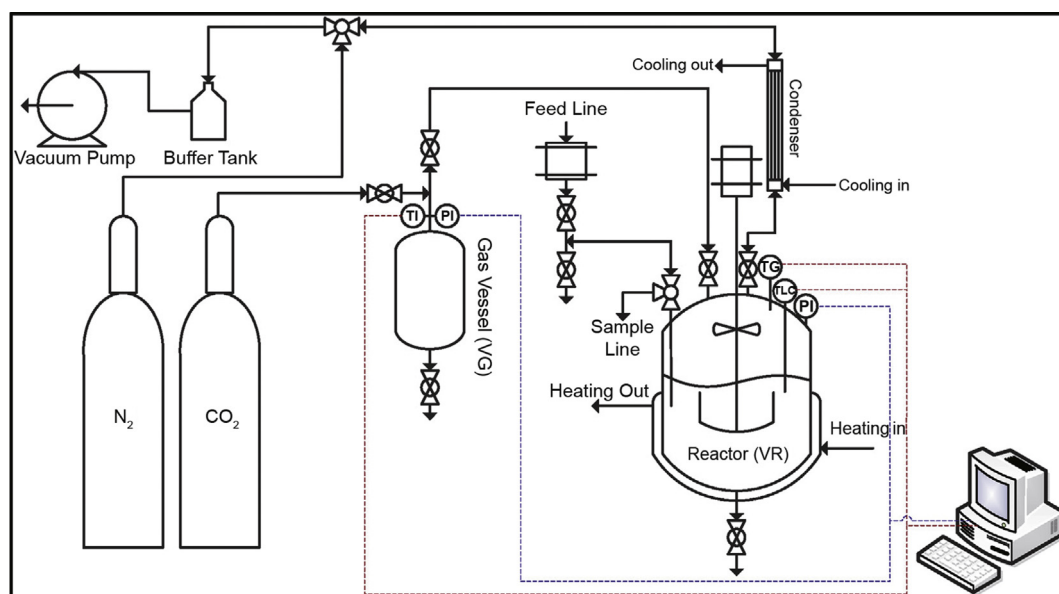Fig. 4. Vapor-liquid equilibrium apparatus for atmospheric pressure.

Fig. 5. Medium pressure vapor–liquid equilibria apparatus.

$p_{Solvent}^{T_{Cond}}$ is the vapor pressure of the solvent at the temperature after the condensers. The vapor pressure of solvent was measured in the medium pressure VLE apparatus.

Medium pressure (high temperature) VLE apparatus: The apparatus in Fig. 5 consists of a jacketed reactor (glass or steel reactor), a mechanical stirrer, two Pt-100 temperature sensors for measurement of liquid and gas phase temperatures ($\pm 0.02°C$), and three pressure transducers for accurate pressure measurements: PTX5072 ($0–600 \pm 0.3$ kPa), PTX517 ($0–200 \pm 0.2$ kPa) and PTX5022 ($0–10 \pm 0.01$ kPa). An SS-316 gas tank is used to add CO_2 to the reactor in batches. The pressure and temperature in the tank are measured using a Pt-100 temperature sensor and a PTX 610 pressure transducer ($0–600 \pm 0.6$ kPa). A Julabo ME6 heat circulator using ethylene glycol as a heating medium controls

the temperature in the reactor. Two silicon heating tapes are used to minimize heat loss through the reactor lid. Data logging is done using a Lab-view program via a National Instrument NI-4903 module [45].

The experiments were started with the evacuation of the reactor using a rotary vane pump (Pfeiffer DUO5MC) down to ~0.5 kPa. Approximately 500 mL of unloaded solution was charged into the reactor and the exact weight of the solution added to the reactor was measured. The solution in the reactor was then evacuated for a short time to remove any dissolved gas in the solution, and the desired temperature was set. The system was left to reach equilibrium which was assumed to be reached when gas and liquid temperatures (T_G and T_L) and pressure (P_R) in the reactor were constant for at least 15 min. After equilibrium the temperature was increased (vapor

pressure measurement) or CO_2 was added in small steps from the CO_2 gas tank.

Partial pressure of CO_2 in the reactor was calculated from the total pressure measurements (P_R) assuming that partial pressure of the solvent (P_S) remained constant during the isothermal experiment [46]:

$$p_{CO_2}(kPa) \cong P_R - P_S \tag{3}$$

The amount of CO_2 added to reactor was calculated from the pressure drop in the CO_2 tank using the Peng–Robinson equation of state [47]:

$$n_{CO_2}^{added}(mol) = \frac{V_V}{R \bullet T_V} \bullet \left[\frac{P_V^{Initial}}{Z_{Initial}} - \frac{P_V^{Final}}{Z_{Final}} \right] \tag{4}$$

The amount of CO_2 accumulated in the reactor gas phase at each loading was estimated from:

$$n_{CO_2}^{gas\ phase}(mol) = \frac{P_{CO_2} \bullet V_G}{R \bullet T_G \bullet Z_{CO_2}} \tag{5}$$

Where the gas phase volume, V_G, is calculated as the difference between the volume of the reactor V_R and the solvent volume V_S at experimental temperature. As seen from the equations above the loading was based on the mass balance. However, a sample was then taken after the last equilibrium point and a liquid analysis was performed to ensure that the mass balance calculations were accurate. The solvent volume was calculated using a density of 30 wt% MEA.

2.4. Liquid analyses

The CO_2 concentration of the samples was determined by precipitation with $BaCl_2$, dissolving $BaCO_3$ with excess HCl and back titration with NaOH [37]. Total alkalinity of the solutions was determined by acid titration with 0.1 M H_2SO_4 [37].

2.5. Modelling

2.5.1. VLE modelling

Antoine equation was used to express the partial pressures of unloaded solutions except in case of 30 wt% MEA where the Riedel parameters from Kim et al. (2008) for pure solvent were used in combination with Dalton's law. The constants for Antoine equations were found by fitting the temperature-pressure profiles obtained in the HP apparatus for unloaded solvents.

$$P = 10^{A - \frac{B}{C+T}} \tag{6}$$

The partial pressure of CO_2 in the loaded systems was fitted to a simple mathematical function similar to that of Brúder et al. (2011).

$$pCO_2 = \exp(k_7 \cdot \ln(\alpha) + A + \frac{10}{(1 + B \cdot \exp(-C \cdot \ln(\alpha)))} \tag{7}$$

where

$$A = \frac{k_1}{T} + k_2 \tag{8}$$

$$B = \exp\left(\frac{k_3}{T} + k_4\right) \tag{9}$$

$$C = \frac{k_5}{T} + k_6 \tag{10}$$

2.5.2. Estimation of the heat requirement of the solvent regeneration

Both the thermal and electrical energy should be taken into account to evaluate the overall energy requirement. Brúder et al. [48] used equivalent work to take into account the thermal energy used in the reboiler, the electricity used in alternative process configurations like LVR, and the electricity used in the compression of the product CO_2. This enabled the benefits of higher reboiler pressure to be studied. However, in this work, since data are only available up to 120 °C, we estimate the heat requirement of the new solvent systems assuming similar reboiler pressures for all studied systems and basic process configuration. This makes it possible to compare reboiler duties using the method described in [14].

The heat requirement (kJ $mol_{CO_2}^{-1}$) in the reboiler can be estimated using the following equations:

$$Q_{req} = Q_{Desorption} + Q_{strip} + Q_{sens} \tag{11}$$

$$Q_{Desorption} = -\Delta H_{abs\ CO_2} \tag{12}$$

$$Q_{Sens} = \frac{\rho c_{p,amine} \Delta T}{(\alpha_{rich} - \alpha_{lean}) C_{Amine}} \tag{13}$$

$$Q_{Strip} = \frac{n_{H_2O,top} \Delta H_{H_2O}^{vap}}{n_{CO_2,top}} = \frac{p_{sol}^{Sat}(T_{Top,Reg})}{p_{CO_2}(T_{Top,Reg}\alpha_{Rich})} \Delta H_{H_2O}^{vap} \tag{14}$$

In the equations, $Q_{Desorption}$, Q_{strip} and Q_{sens} (kJ $mol_{CO_2}^{-1}$) are the heat of desorption, the heat of stripping and sensible heat [14]. $\Delta H_{abs\ CO_2}$ is the heat of absorption (kJ $mol_{CO_2}^{-1}$), p_{sol}^{Sat} (kPa) is the saturation pressure of solvent at the temperature at the top of the regenerator ($T_{Top,Reg}$), α_{rich} is the rich loading, p_{CO_2} (kPa) is the partial pressure of CO_2 at the top of the regenerator, and $\Delta H_{H_2O}^{vap}$ (kJ mol_{steam}^{-1}) is the heat of vaporization. ρ is density (kg m^{-3}), Cp is the heat capacity (kJ kg K^{-1}), ΔT is the difference between the lean and rich solvent temperatures at the hot side of the cross heat exchanger (K), C_{Am} is the amine concentration ($mol_{amine}\ m^{-3}$), and $\alpha_{rich} - \alpha_{lean}$ is the cyclic capacity ($mol_{CO_2}\ mol_{amine}^{-1}$). The equations are the same as in H. Kim, S.J. Hwang and K.S. Lee [14] except that the effect of gaseous CO_2 is neglected. The vapor pressure at the top of the stripper is the measured vapor pressure of the studied solvent systems. H. Kim, S.J. Hwang and K.S. Lee [14] used vapor pressure of water combined with Raoult's law. The heat of absorption/desorption in Eq. 12 is estimated using VLE data and the Gibbs–Helmholtz equation [14].

The rich amine solution is preheated by the cross heat exchanger with the lean amine solution. However, it cannot be heated to reboiler temperature. This is a process determined heat loss, assuming that desorption does not occur in the heat exchanger. This is presented in Equation (13) and Cp is assumed to be equal to that of 30 wt% MEA value for all blends, the solvent density was estimated to be 1 kg L^{-1} and ΔT was chosen to be 10 °C. The rich loading is determined by assuming that the solvent would be in equilibrium with a CO_2 concentration of 9.5 kPa at the bottom of the absorber (40 °C). Similarly the lean loading is taken assuming that the solvent is in equilibrium with 20 kPa CO_2 at reboiler temperature.

The reboiler temperature is estimated using the following equation taking into account that the total pressure is fixed to 1.9 bar (P$_{tot}$)

$$P_{tot} = P_{CO_2}(\alpha_{lean}, T_{reboiler}) + P_{H_2O+solvent}(T_{reboiler}) \tag{15}$$

Iteration is needed to solve the equation. However, for all the studied systems the reboiler temperature is very close to 120 °C.

Equation (14) describes the energy consumed to drive CO_2 through the column using steam. The gas mixture leaving the regenerator therefore contains a significant fraction of water vapor which needs to be condensed and returned to the process. As in the reboiler, at the top of the desorber the CO_2 partial pressure and temperature are found by iteration assuming that there is no pressure drop in the regeneration.

3. Results and discussion

3.1. Screening experiments

The cyclic capacities of the studied systems are shown in Fig. 6. Fig. 7 shows the lean and rich loadings during the screening experiments. 30 wt% MEA was tested as a reference. The cyclic capacity is 1.1 mol kg^{-1} and it is slightly higher than the cyclic capacities reported in [11] (0.82 mol kg^{-1} solvent) but is in good agreement with the VLE model by [49] (1.2 mol kg^{-1} solvent).
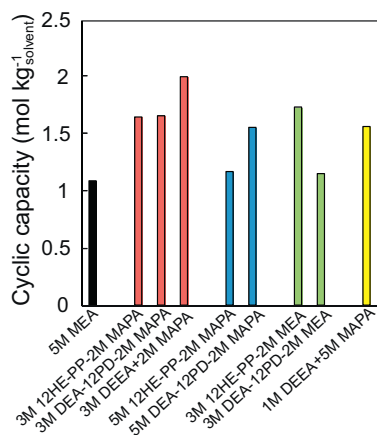

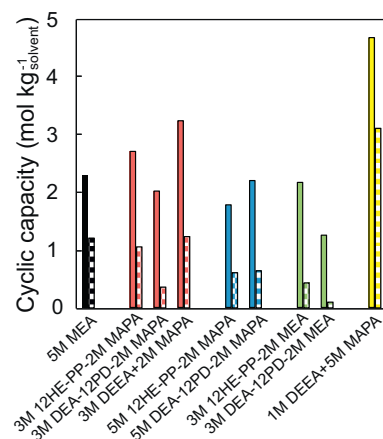Fig. 6. The cyclic capacity of the tested blends. 5M MEA was tested as reference.

Fig. 7. Lean and rich loadings during the screening experiments.

Fig. 6 shows that all the blends with 3M tertiary amine and 2M MAPA performed much better than 5M MEA (the three red bars on the left hand side). The best performance was seen with 3M DEEA + 2M MAPA, 80% higher cyclic capacity compared to 5M MEA. Also both 3M 12HE-PP and 3M DEA-12PD blended with 2M MAPA showed high cyclic capacity, more than 50% higher compared to 5M MEA. 2M MAPA-3M DEEA blend reaches high loading during absorption at 40 °C (rich loading) with lean loading close to that of 30 wt% MEA as shown in Fig. 7. The lean and rich loadings of these three blends are very different. However, all of them have at least 50% better cyclic capacity compared to 30 wt% MEA and the blend 2M MAPA blend with 3M DEA-12PD reaches rich loading lower than that of 30 wt% MEA. However, due to a low lean loading the cyclic capacity is very high. These results underline that screening experiments to identify solvent blends with high potential should always include desorption tests. Increasing the amount of tertiary amine from 3M to 5M did not increase the performance as can be seen by the blue bars (5M 12HE-PP-2M MAPA and 5M DEA-12PD-2M MAPA) in Fig. 7.

As also seen in Fig. 6 promoting DEA-12PD with 2M MEA performs similarly to 30 wt% MEA. However, when 12HE-PP is blended with 2M MEA the performance is much better. Looking at the lean and rich loadings Fig. 7, we can see that the lean loadings for these two systems are very similar and the greatest difference is the rich loading that was higher for 3M DEA-12PD + 2M MEA system compared to 3M 12HE-PP + 2M MEA. Conway et al. [33] concluded that the cyclic capacity of 3M DEEA+2M MEA was over 50% higher compared to what they estimated for 5M MEA which is similar as seen for the blend of DEA12-PD and MEA. The pKa values of the three tertiary amines, 12HE-PP, DEA-12PD and DEEA, are similar, 9.57, 9.69 and 9.87, respectively. Nevertheless, the performance seems to increase with increasing pKa. The cyclic capacity of the 12HEP-PP, DEA-12PD when blended with MAPA is very similar indicating that the pKa of the tertiary amine cannot alone explain the results.

Finally, one additional system was tested. Based on preliminary results by [50] adding 1M DEEA to 5M MAPA
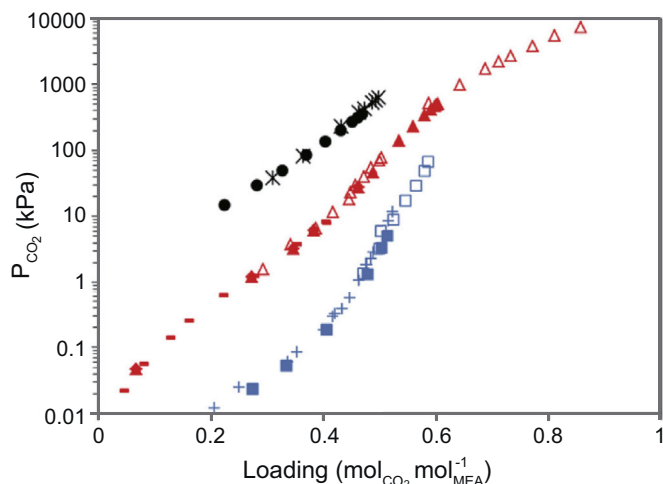
Fig. 8. Vapor-liquid equilibrium of 5M MEA compared to the literature. ■ This work, 40 °C; ▲ This work, 80 °C; ● This work, 120 °C; □ by [51] 40 °C; + by [42], 40 °C; ■ by [42], 80 °C; △ by [51], 80 °C; ✳ by [42], 120 °C.

Fig. 9. Vapor pressure above the unloaded blends. ■ 5M MAPA + 1M DEEA, ◇ 2M MAPA + 3M DEEA, ✳ 2M MAPA + 3M DEA-12PD, △ 2M MEA + 3M 12HE-PP and + 2M MAPA + 3M 12HE-PP. Lines (−) Antoine equation using parameters in Table 2.

increased the cyclic capacity significantly. The 1M DEEA+5M MAPA was screened to study this further. We can see that the system reaches very high lean loading (Fig. 7). This is not that surprising based on the literature data for single MAPA systems in Fig. 1 which found high rich loadings. However, the screening experiment performed in this study shows that by just adding 1M DEEA, the cyclic capacity increases from 0.2 to 0.5 mol kg^{-1} reported for 2–3.5M MAPA, see Fig. 2, to 1.6 mol kg^{-1} as seen in Fig. 7.

Based on the screening experiments the following systems were chosen for equilibrium studies:

- DEEA, 12HE-PP and 12PD blended with 2M MAPA due to the high cyclic capacities.
- 3M 12HE-PP promoted with MEA, showing a high cyclic capacity
- 1M DEEA blended with 5M MAPA. The system had unexpected behavior since the addition of 1M DEEA seems to greatly increase the cyclic capacity compared to single MAPA systems.

3.2. VLE of 5M MEA

Vapor-liquid equilibrium experiments were performed with 30 wt% MEA to ensure correct performance of the equilibrium equipment. The results are presented in Fig. 8 where the data agree very well with literature data [42,51]. Since data at 80 °C were measured with two different experimental apparatuses (low pressure apparatus and medium pressure apparatus) we could also ensure good consistency between the apparatuses.

3.3. Vapor pressure of the unloaded systems

The vapor pressures of the unloaded solutions are shown in Fig. 9 where the vapor pressures are fairly similar for all the studied systems. 5M MAPA +1M DEEA has the lowest vapor pressure and 2M MAPA + 3M DEEA has the
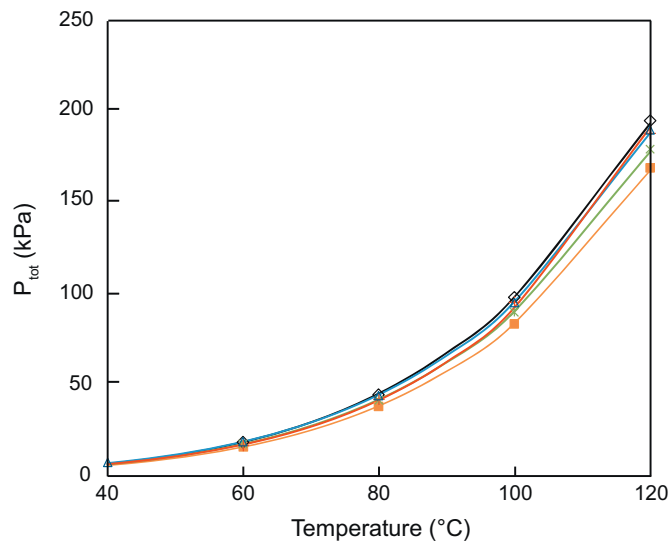
highest. The difference is 15% at 120 °C. The data were fitted to the Antoine equation and the constants together with AARD are shown in Table 2. The Antoine equation is able to represent the data very well with AARD below 3% for all the blends.

3.4. VLE of the loaded systems

The measured and modelled partial pressure of CO_2 of the studied systems is shown in Fig. 10. The parameters and the average standard deviation for the VLE models are given in Table 3. The experiments at 40 °C were performed twice for all other systems than 2M MAPA + 3M 12HE-PP. In general the repeated experiments agreed very well as seen in Fig. 11. However, when it comes to 2M MAPA + 3M DEA-12PD there is slight disagreement. The reason for this change is unknown since both sets were performed using the same procedures. The model was fitted using 80 °C, 120 °C data as well as the 40 °C data which showed higher partial pressures of CO_2 to ensure that the final evaluation does not overestimate the performance of 2M MAPA + 3M DEA-12PD system.

Due to formation of two liquid phases at high loadings of 2M MAPA + 3M 12HE-PP, it was not possible to use the low temperature VLE equipment. To get some VLE data at 40 °C,

Table 2
Fitted Antoine parameters for the studied systems. Antoine equation $P = 10^{A - \frac{B}{C + T}}$, where T is in K and P in kPa.

	A	B	C	AARD [%]
5M MAPA +1M DEEA	7.1958	1742.747	−42.6056	2.28
2M MAPA + 3M DEEA	6.6826	1399.255	−74.8477	2.62
2M MAPA + 3M DEA-12PD	6.8894	1555.698	−57.8145	1.79
2M MEA + 3M 12HE-PP	7.1345	1702.697	−42.7843	2.88
2M MAPA + 3M 12HE-PP	8.7844	2807.482	38.5888	2.91
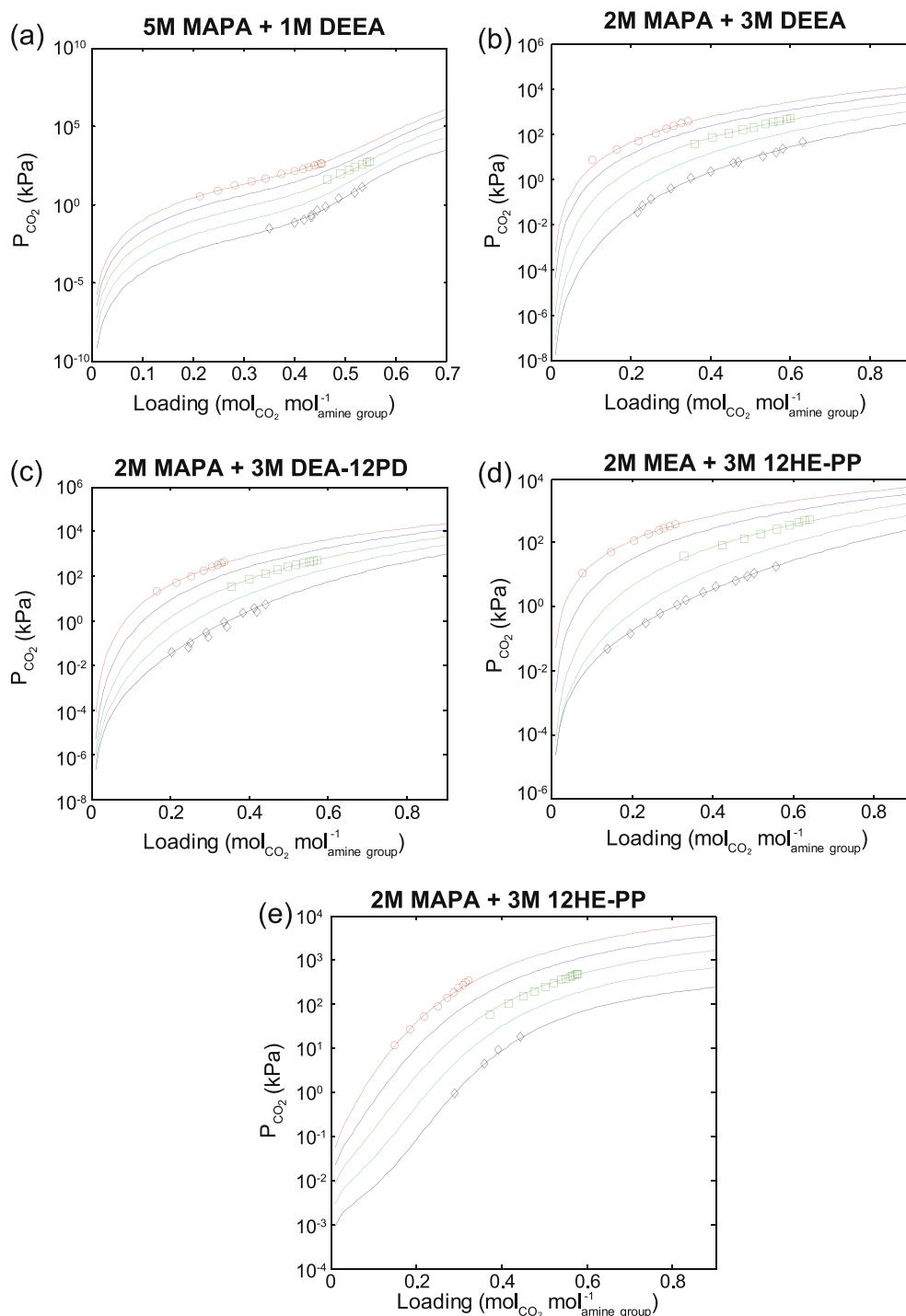
Fig. 10. Vapor-liquid equilibrium (a) 5M MAPA + 1M DEEA, (b) 2M MAPA + 3M DEEA, (c) 2M MAPA + 3M DEA-12PD (d) 2M MEA + 3M 12HE-PP and (e) 2M MAPA + 3M 12HE-PP. ◇ This work 40 °C; ▢ This work 80 °C; ○ This work 120 °C, ─ soft model 40 °C; ─ soft model 60 °C; ─ soft model 80 °C; ─ soft model 100 °C; ─ soft model 120 °C.

the screening equipment was used to provide four equilibrium points in a similar way as previously done by [52].

3.5. Comparison of cyclic capacities based on the VLE models and the screening experiments

Fig. 11 shows the cyclic capacity calculated for the different systems for temperatures between 40 °C and 120 °C.

As mentioned in Section 2.5.2 the rich loading is determined by assuming that the solvent would be in equilibrium with CO_2 concentration of 9.5 kPa in the bottom of the absorber (40 °C). Similarly the lean loading is taken assuming that the solvent is in equilibrium with 20 kPa CO_2 at the reboiler temperature. In the same figure the cyclic capacities based on the screening work presented in Fig. 6 is also plotted. In the screening experiments, the rich loading is determined when

Table 3
The parameters in Equation (7) for 5M MAPA + 1M DEEA, 2M MAPA + 3M DEEA, 2M MAPA + 3M DEA-12PD, 2M MAPA + 3M 12HE-PP and 2M MEA + 3M 12HE-PP systems.

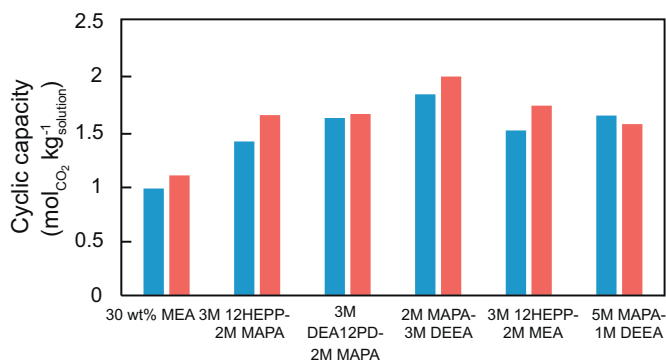|	k_1	k_2	k_3	k_4	k_5	k_6	k_7	AARD [%]
5M MAPA +1M DEEA	−11912.9	38.932	−2316.01	2.6958	1846.848	1.7726	4.7748	18.9
2M MAPA + 3M DEEA	−3242.08	9.3121	1412.618	−5.5633	1544.628	−3.8736	3.7009	17.6
2M MAPA + 3M DEA-12PD	−3283.23	10.7401	667.3821	−3.137	1781.925	−4.11	3.4023	7.6
2M MAPA + 3M 12HE-PP	−6151.7728	15.77805	−1412.4344	1.4380	1782.2034	−3.1013	0.6854	7.1
2M MEA + 3M 12HE-PP	975.4063	−1.4761	2275.969	−7.124	2109.224	−5.4333	2.6766	8.0

Fig. 11. The cyclic capacity calculated using the VLE models and screening. Blue columns: VLE data between 40 °C and 120 °C, red columns: screening data at 40 °C and 80 °C.

the gas outlet concentration showed 9.5% (~9.5 kPa) at 40 °C. The lean loading was reached by bubbling nitrogen through the solution until the CO_2 analyzer showed 1.0% CO_2 (~1 kPa) at 80 °C.

Average deviation between these two methods, shown in Fig. 11, for the studied systems is 11%, which can be considered to be acceptable agreement since the lean loadings are determined at different temperatures and since one set of data is in equilibrium and the other is based on screening. Based on the data, it might be argued that the

screening setup seems to give somewhat higher cyclic capacities compared to what is seen based on the equilibrium experiments. This is true for five out of the six systems studied here. The only system that does not follow this trend is 5M MAPA - 1M DEEA.

This exercise illustrates that fast solvent screening can be used to identify solvents with potential. But it is important to remember that one should have careful control over the amount of CO_2 absorbed and liquid analyses should be used as discussed in [7]. Using the temperature difference between 40 °C and 80 °C seems to be acceptable, as long as the solvents are stripped down to 0.1 kPa CO_2 at 80 °C, even though a better approach would be to screen solvents in more realistic conditions. However, the deviations are around 10% and this should be taken into account when deciding which solvents should be chosen for further studies.

3.6. Estimation of reboiler duty

The short-cut method presented in Section 3.2.2 was used to estimate the required thermal energy in the reboiler. The results are shown in Fig. 12. The short-cut method gave energy consumption of 3.5 MJ $kg_{CO_2}^{-1}$ for 30 wt% MEA which agrees with literature [14]. The value is also in good agreement with experimental pilot data from several pilots connected to coal-fired power plants reporting reboiler
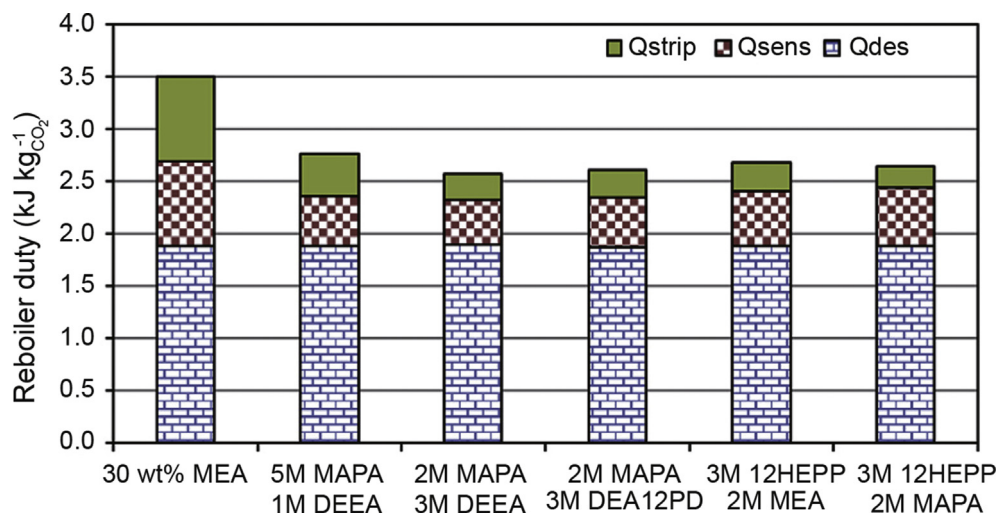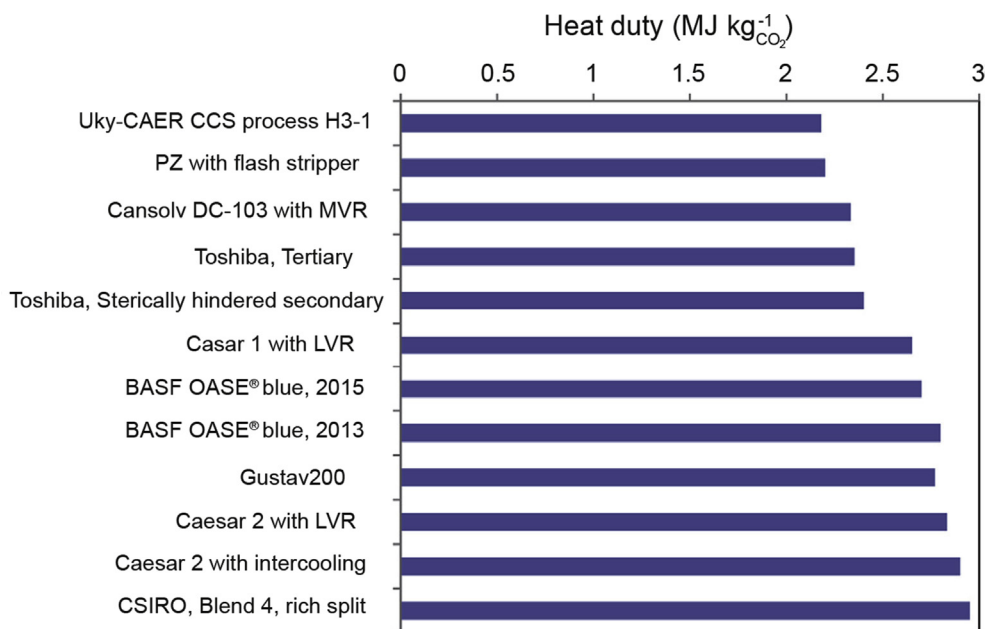

Fig. 12. Estimated reboiler duty.

Fig. 13. Experimental heat duties of novel solvents. References: Uky-CAER CCS process H3-1 [62], PZ with flash stripper [65]; Cansolv DC-103 with LVR [63]; Toshiba, tertiary and Toshiba, Sterically hindered secondary [64]; Cesar 1 with LVR, Cesar 2 with LVR, Cesar 2 with intercooling [56]; BASF OASE® blue, 2013 [59]; BASF OASE® blue, 2015 [61]; Gustav200 [60]; CSIRO, Blend 4, rich split [55].

duties between 3.5 and 3.6 MJ $kg_{CO_2}^{-1}$ [53–58]. The new solvent blends evaluated in this work had energy consumption between 2.5 and 2.76 MJ $kg_{CO_2}^{-1}$. Even though, the thermal energy requirement of 2.5 MJ $kg_{CO_2}^{-1}$ is almost 30% lower than the energy consumption of the chosen base case (30 wt% MEA), the performance of the analyzed solvents not better compared to many other proposed solvents systems experimentally tested under real process conditions. Fig. 13 shows that reboiler duties of the novel solvent systems tested in the resent years have often been between 2.6 and 3.0 MJ $kg_{CO_2}^{-1}$ [55,56,59–61]. Only three references were found with pilot data with real flue gas with energy consumptions lower than 2.5 MJ $kg_{CO_2}^{-1}$ [62–64]. Additionally, [65] reported that with an advanced stripper configuration the energy consumption of Piperazine solvent can be reduced below 2.5 MJ $kg_{CO_2}^{-1}$. All the campaigns with energy consumption below 2.5 MJ $kg_{CO_2}^{-1}$ except those reported by [64] include process improvements or heat integration explaining partly the low energy consumption of these campaigns.

The main energy requirement comes from reversing the reaction that is responsible for almost 2 MJ $kg_{CO_2}^{-1}$ in the case of 2M MAPA + 3M DEEA, 2M MAPA + 3M DEA12PD and 3M 12HEPP + 2M MEA. The heat of reaction for these solvents is similar to that of 30 wt% MEA and the main reduction in the heat consumption comes from increased cyclic capacity, Fig. 11 gives a lower sensible heat and increased partial pressure of CO_2 in the stripper which reduces the need for stripping steam. The short-cut method indicates a very small stripping steam requirement, only around 10% of the total heat

requirement. The sensible heat requirement of the solvent uses 15–20% of the total energy in the case of 2M MAPA + 3M DEEA, 2M MAPA + 3M DEA12PD and 3M 12HEPP + 2M MEA.

4. Conclusions

The potential of five blends of tertiary amines promoted with primary amine were experimentally studied by testing the solvents first with screening equipment followed by the measurement of the vapor–liquid equilibria. In addition, three of the solvent blends showed reboiler duties below 2.6 MJ $kg_{CO_2}^{-1}$ when a so-called 'short-cut method' was used. The energy consumption is similar to new solvent aqueous blends published in literature. In future studies the chemical stability under process conditions should be addressed. High solvent stability is required, due to the high solvent cost.

Acknowledgments

Appendix A. Supplementary data

Supplementary data to this article can be found online at https://doi.org/10.1016/j.gee.2019.01.007.

Appendix.

Table A1
Vapor pressures above the tested solutions.

5M MAPA	T [°C]	30	39.99	60	79.95	99.98	120
+1M DEEA	P [kPa]	3.152	5.859	15.718	37.94	83.242	168.931
2M MAPA	T [°C]	30	39.99	59.95	79.94	99.99	120
+ 3M DEEA	P [kPa]	3.5	6.712	18.336	44.379	97.885	194.901
2M MAPA	T [°C]	30	39.97	59.96	80	99.99	120
+ 3M DEA-12PD	P [kPa]	3.481	6.394	17.363	41.425	89.71	179.31
2M MAPA	T [°C]	29.99	39.98	60	80	100	120
+ 3M 12HE-PP	P [kPa]	3.712	6.417	16.511	41.925	95.2	187.954
2M MEA	T [°C]	30	40	59.96	79.95	100	120
+ 3M 12HE-PP	P [kPa]	3.841	7.156	18.517	43.918	95.01	189.931

Table A2
CO_2 solubility data for 30 mass % MEA based on LP and HP experiments.

40 °C		80 °C		120 °C	
$\alpha\ CO_2$ (mol mol^{-1})	pCO_2 (kPa)	$\alpha\ CO_2$ (mol mol^{-1})	pCO_2 (kPa)	$\alpha\ CO_2$ (mol mol^{-1})	pCO_2 (kPa)
LP		*HP*		*HP*	
0.513	5.08	0.488	46.8	0.224	15.1
0.503	3.33	0.535	139.2	0.282	29.8
0.478	1.34	0.56	232.6	0.327	50.2
0.406	0.19	0.58	339.6	0.369	86.0
0.334	0.05	0.591	410.3	0.404	136.5
0.274	0.02	0.599	469.5	0.431	200.9
		0.601	488.7	0.451	270.6
		0.603	506.4	0.461	316.7
		LP		0.469	353.7
		0.462	27.87		
		0.383	6.19		
		0.346	3.26		
		0.273	1.20		
		0.067	0.05		

Table A3
CO_2 solubility data for 2M MAPA with 3M DEEA based on LP and HP experiments.

40 °C		80 °C		120 °C	
αCO_2 (mol mol^{-1})	pCO_2 (kPa)	$\alpha\ CO_2$ (mol mol^{-1})	pCO_2 (kPa)	$\alpha\ CO_2$ (mol mol^{-1})	pCO_2 (kPa)
LP		*HP*		*HP*	
0.217	0.04	0.359	36.6	0.103	7.1
0.23	0.07	0.405	72.3	0.164	21.1
0.25	0.14	0.445	114.7	0.219	49.1
0.3	0.41	0.481	161.8	0.262	104.6
0.35	1.14	0.506	201.3	0.288	171.9
0.4	2.27	0.538	274.0	0.307	225.6
0.456	5.33	0.557	334.5	0.327	313.7
0.53	10.86	0.572	389.6	0.342	387.5
0.58	23.06	0.591	480.6		
0.63	44.52	0.599	526.6		
0.47	*5.92*				
0.565	*15.79*				

Table A4
CO_2 solubility data for 5M MAPA with 1M DEEA based on LP and HP experiments.

40 °C		80 °C		120 °C	
αCO_2 (mol mol^{-1})	pCO_2 (kPa)	αCO_2 (mol mol^{-1})	pCO_2 (kPa)	αCO_2 (mol mol^{-1})	pCO_2 (kPa)
LP		*HP*		*HP*	
0.533	13.40	0.465	39.2	0.214	3.2
0.518	5.34	0.491	90.1	0.249	7.3
0.444	0.40	0.507	159.1	0.281	16.2
0.434	0.16	0.518	225.1	0.314	28.8
0.399	0.07	0.533	367.2	0.343	47.2
0.35	0.03	0.542	470.9	0.374	83.1
0.486	*2.42*	0.547	550.8	0.4	131.2
0.46	*0.72*			0.417	184.5
0.433	*0.22*			0.427	229.8
0.418	*0.10*			0.438	290.6
				0.446	346.7
				0.452	400.0
				0.454	414.2

Table A5
CO_2 solubility data for 2M MAPA with 3M DEA-12PD based on LP and HP experiments.

40 °C		80 °C		120 °C	
αCO_2 (mol mol^{-1})	pCO_2 (kPa)	αCO_2 (mol mol^{-1})	pCO_2 (kPa)	αCO_2 (mol mol^{-1})	pCO_2 (kPa)
LP		*HP*		*HP*	
0.204	0.04	0.354	34.6	0.165	20.7
0.251	0.11	0.399	74.4	0.215	52.2
0.291	0.32	0.441	131.7	0.254	103.4
0.335	0.89	0.472	189.8	0.284	178.5
0.384	2.32	0.498	249.2	0.305	253.5
0.413	3.69	0.519	311.5	0.32	321.5
0.441	5.26	0.537	371.9	0.33	376.7
0.245	*0.07*	0.552	434.3	0.335	405.3
0.295	*0.19*	0.562	478.4		
0.342	*0.52*	0.57	518.8		
0.418	*2.57*				

Table A6
CO_2 solubility data for 2M MEA with 3M 12HE-PP based on LP and HP experiments.

40 °C		80 °C		120 °C	
αCO_2 (mol mol^{-1})	pCO_2 (kPa)	αCO_2 (mol mol^{-1})	pCO_2 (kPa)	αCO_2 (mol mol^{-1})	pCO_2 (kPa)
LP		*HP*		*HP*	
0.138	0.05	0.328	38.4	0.076	11.2
0.195	0.15	0.424	82.7	0.149	51.9
0.233	0.32	0.478	137.7	0.205	118.3
0.312	1.19	0.518	192.7	0.24	184.2
0.377	2.80	0.56	272.3	0.268	257.9
0.457	6.27	0.591	351.0	0.28	292.1
0.503	11.06	0.614	432.1	0.293	332.6
0.556	18.80	0.629	484.5	0.308	386.9
0.27	*0.62*	0.641	538.6		
0.334	*1.65*				
0.408	*4.15*				
0.486	*9.08*				

Table A7
CO_2 solubility data for 2M MAPA with 3M 12HE-PP

40 °C		80 °C		120 °C	
αXO_2	pCO_2	αXO_2	pCO_2	αXO_2	pCO_2
(mol mol^{-1})	(kPa)	(mol mol^{-1})	(kPa)	(mol mol^{-1})	(kPa)
LP - screening setup		*HP*		*HP*	
0.289	0.9	0.334	43.8	0.148	11.7
0.359	4.5	0.373	56.9	0.185	26.5
0.392	9.0	0.416	106.1	0.219	51.5
0.444	18.0	0.45	154.6	0.25	90.0
		0.475	198.0	0.272	139.0
		0.502	253.6	0.288	187.3
		0.522	303.8	0.299	232.9
		0.539	356.9	0.309	276.8
		0.55	390.9	0.316	315.5
		0.56	423.0	0.321	343.7
		0.566	445.9		
		0.571	465.2		
		0.576	483.0		
		0.579	498.5		

References

[1] Iea, Key World Energy Statistics 2013, 2013. http://www.iea.org/publications/freepublications/publication/key-world-energy-statistics-2013.html.

[2] H.F. Svendsen, E.T. Hessen, T. Mejdell, Chem. Eng. J. 171 (2011) 718–724.

[3] F.A. Chowdhury, H. Yamada, T. Higashii, K. Goto, M. Onoda, Ind. Eng. Chem. Res. 52 (2013) 8323–8331.

[4] M.W. Arshad, P.L. Fosbøl, N. Von Solms, H.F. Svendsen, K. Thomsen, J. Chem. Eng. Data 58 (2013) 1974–1988.

[5] B.A. Oyenekan, G.T. Rochelle, AIChE J. 53 (2007) 3144–3154.

[6] P. Brúder, F. Owrang, H.F. Svendsen, Int. J. Greenh. Gas Con. 11 (2012) 98–109.

[7] I.M. Bernhardsen, H.K. Knuutila, Int. J. Greenh. Gas Con. 61 (2017) 27–48.

[8] M.W. Arshad, H.F. Svendsen, P.L. Fosbøl, N. Von Solms, K. Thomsen, J. Chem. Eng. Data 59 (2014) 764–774.

[9] Y.E. Kim, S.J. Moon, Y.I. Yoon, S.K. Jeong, K.T. Park, S.T. Bae, S.C. Nam, Sep. Purif. Technol. 122 (2014) 112–118.

[10] G. Puxty, R. Rowland, A. Allport, Q. Yang, M. Bown, R. Burns, M. Maeder, M. Attalla, Environ. Sci. Technol. 43 (2009) 6427–6433.

[11] A. Hartono, S.J. Vevelstad, A. Ciftja, H.K. Knuutila, Int. J. Greenh. Gas Con. 58 (2017) 201–211.

[12] N. El Hadri, D.V. Quang, E.L.V. Goetheer, M.R.M. Abu Zahra, Appl. Energy 185 (2016) 1433–1449.

[13] J.G.M.S. Monteiro, D.D.D. Pinto, S.A.H. Zaidy, A. Hartono, H.F. Svendsen, Int. J. Greenh. Gas Con. 19 (2013) 432–440.

[14] H. Kim, S.J. Hwang, K.S. Lee, Environ. Sci. Technol. 49 (2015) 1478–1485.

[15] K. Klepáčová, P.J.G. Huttenhuis, P.W.J. Derks, G.F. Versteeg, J. Chem. Eng. Data 56 (2011) 2242–2248.

[16] A. Hartono, F. Saleem, M.W. Arshad, M. Usman, H.F. Svendsen, Chem. Eng. Sci. 101 (2013) 401–411.

[17] M. Garcia, H.K. Knuutila, S. Gu, Green Energy Environ. 1 (2016) 246–257.

[18] M.W. Arshad, N. Von Solms, K. Thomsen, Int. J. Greenh. Gas Con. 53 (2016) 401–424.

[19] I. Kim, H.F. Svendsen, Int. J. Greenh. Gas Con. 5 (2011) 390–395.

[20] B. Xu, H. Gao, X. Luo, H. Liao, Z. Liang, Int. J. Greenh. Gas Con. 51 (2016) 11–17.

[21] J.G.M.S. Monteiro, H. Majeed, H. Knuutila, H.F. Svendsen, Chem. Eng. Sci. 129 (2015) 145–155.

[22] J. Li, A. Henni, P. Tontiwachwuthikul, Ind. Eng. Chem. Res. 46 (2007) 4426–4434.

[23] R.J. Littel, W.M.P. Van Swaaij, G.F. Versteeg, AIChE J. 36 (1990) 1633–1640.

[24] J.G.M.S. Monteiro, H. Knuutila, N.J.M.C. Penders-Van Elk, G. Versteeg, H.F. Svendsen, Chem. Eng. Sci. 127 (2015) 1–12.

[25] D.D.D. Pinto, CO_2 Capture Solvents: Modeling and Experimental Characterization, Norwegian University of Science and Technology (NTNU), 2014.

[26] J.G.M.S. Monteiro, S. Hussain, H. Majeed, E.O. Mba, A. Hartono, H. Knuutila, H.F. Svendsen, AIChE J. 60 (2014) 3792–3803.

[27] J. Li, H. Liu, Z. Liang, X. Luo, H. Liao, R. Idem, P. Tontiwachwuthikul, Chem. Eng. J. 270 (2015) 485–495.

[28] D.D.D. Pinto, H. Knuutila, G. Fytianos, G. Haugen, T. Mejdell, H.F. Svendsen, Int. J. Greenh. Gas Con. 31 (2014) 153–164.

[29] H.K. Knuutila, Å. Nannestad, Int. J. Greenh. Gas Con. 61 (2017) 94–103.

[30] P.D. Vaidya, E.Y. Kenig, in: G.V.R. Reklaitis, M.M. El-Halwagi (Eds.), Proceedings of the 1st Annual Gas Processing Symposium, vol. 1, Elsevier, Amsterdam, 2009, pp. 239–246.

[31] P.B. Konduru, P.D. Vaidya, E.Y. Kenig, in: Proceedings of the 2nd Annual Gas Processing Symposium, vol. 2, Elsevier, Amsterdam, 2010, pp. 21–29.

[32] P. Brœder, H.F. Svendsen, Energy Procedia 23 (2012) 45–54.

[33] W. Conway, S. Bruggink, Y. Beyad, W. Luo, I. Melián-Cabrera, G. Puxty, P. Feron, Chem. Eng. Sci. 126 (2015) 446–454.

[34] G.F. Versteeg, L.a.J. Van Dijck, W.P.M. Van Swaaij, Chem. Eng. Commun. 144 (1996) 113–158.

[35] E.F. Da Silva, H.F. Svendsen, Int. J. Greenh. Gas Con. 1 (2007) 151–157.

[36] A. Hartono, A.F. Ciftja, P. Brúder, H.F. Svendsen, Energy Procedia (2014) 2138–2143.

[37] S. Ma'mun, H.F. Svendsen, K.A. Hoff, O. Juliussen, Energy Convers. Manage. 48 (2007) 251–258.

[38] U.E. Aronu, H.F. Svendsen, K.A. Hoff, Int. J. Greenh. Gas Con. 4 (2010) 771–775.

[39] P. Brúder, A. Grimstvedt, T. Mejdell, H.F. Svendsen, Chem. Eng. Sci. 66 (2011) 6193–6198.

[40] U.E. Aronu, K.A. Hoff, H.F. Svendsen, Chem. Eng. Res. Des. 89 (2011) 1197–1203.

[41] S. Ma'mun, J.P. Jakobsen, H.F. Svendsen, O. Juliussen, Ind. Eng. Chem. Res. 45 (2006) 2505–2512.

[42] U.E. Aronu, S. Gondal, E.T. Hessen, T. Haug-Warberg, A. Hartono, K.A. Hoff, H.F. Svendsen, Chem. Eng. Sci. 66 (2011) 6393–6406.

[43] H. Knuutila, E.T. Hessen, I. Kim, T. Haug-Warberg, H.F. Svendsen, Chem. Eng. Sci. 65 (2010) 2218–2226.

[44] U.E. Aronu, S. Gondal, E.T. Hessen, T. Haug-Warberg, A. Hartono, K.A. Hoff, H.F. Svendsen, Chem. Eng. Sci. 66 (2011) 6393–6406.

[45] A. Hartono, R. Rennemo, M. Awais, S.J. Vevelstad, O.G. Brakstad, I. Kim, H.K. Knuutila, Int. J. Greenh. Gas. Cont. 63 (2017) 260–271.

[46] A. Hartono, O. Juliussen, H.F. Svendsen, J. Chem. Eng. Data 53 (2008) 2696–2700.

[47] D.-Y. Peng, D.B. Robinson, Ind. Eng. Chem. Fundam. 15 (1976) 59–64.

[48] G. Rochelle, E. Chen, S. Freeman, D. Van Wagener, Q. Xu, A. Voice, Chem. Eng. J. 171 (2011) 725–733.

[49] P. Brúder, K.G. Lauritsen, T. Mejdell, H.F. Svendsen, Chem. Eng. Sci. 75 (2012) 28–37.

[50] A.F. Ciftja, H.F. Svendsen, H.K. Knuutila, Two phase formation and cyclic capacity of DEEA-MAPA blends, in: 8th Trondheim Conference on CO2 Capture, Transport and Storage TCCS-8, Trondheim, 2015.

[51] M. Wagner, I. Von Harbou, J. Kim, I. Ermatchkova, G. Maurer, H. Hasse, J. Chem. Eng. Data 58 (2013) 883–895.

[52] D.D.D. Pinto, S.a.H. Zaidy, A. Hartono, H.F. Svendsen, Int. J. Greenh. Gas Con. 28 (2014) 318–327.

[53] N. Brigman, M.I. Shah, O. Falk-Pedersen, T. Cents, V. Smith, T. De Cazenove, A.K. Morken, O.A. Hvidsten, M. Chhaganlal, J.K. Feste, G. Lombardo, O.M. Bade, J. Knudsen, S.C. Subramoney, B.F. Fostås, G. De Koeijer, E.S. Hamborg, Energy Procedia 63 (2014) 6012–6022.

[54] A. Cousins, A. Cottrell, A. Lawson, S. Huang, P.H.M. Feron, Greenh. Gases Sci. Technol. 2 (2012) 329–345.

[55] P. Feron, W. Conway, G. Puxty, L. Wardhaugh, P. Green, D. Maher, D. Fernandes, A. Cousins, G. Shiwang, L. Lianbo, N. Hongwei, S. Hang, Energy Procedia 63 (2014) 1399–1406.

[56] J.N. Knudsen, J. Andersen, J.N. Jensen, O. Biede, Energy Procedia 4 (2011) 1558−1565.

[57] J.N. Knudsen, J.N. Jensen, P.-J. Vilhelmsen, O. Biede, Energy Procedia 1 (2009) 783−790.

[58] P. Moser, S. Schmidt, G. Sieder, H. Garcia, T. Stoffregen, Int. J. Greenh. Gas Con. 5 (2011) 620−627.

[59] P. Moser, S. Schmidt, S. Wallus, T. Ginsberg, G. Sieder, I. Clausen, J.G. Palacios, T. Stoffregen, D. Mihailowitsch, Energy Procedia 37 (2013) 2377−2388.

[60] P. Moser, S. Schmidt, G. Sieder, H. Garcia, T. Stoffregen, V. Stamatov, Energy Procedia 4 (2011) 1310−1316.

[61] S.T. Rigby, Results from the Testing on a 1MWel Advanced Aqueous Amine-based PCC Pilot Plant in Wilsonville:, in: 3rd Post Combustion Capture Conference and SaskPower Symposium, Regina, Canada, 2015.

[62] H. Nikolic, K. Liu, Application of a Heat Integrated Post-combustion CO2 Capture System with Hitachi Advanced Solvent into Existing Coal-fired Power Plant, in: 3rd Post Combustion Capture conference., Regina, Canada, 2015.

[63] A. Singh, K. Stéphenne, Energy Procedia 63 (2014) 1678−1685.

[64] S. Saito, M. Udatsu, H. Kitamuraa, S. Murai, Mikawa CO_2 Capture Pilot Plant Test of New Amine Solvent, in: 3rd Post Combustion Capture Conference, Regina Saskatchewan, 2015.

[65] E. Chen, Evaluated Pilot Plant Results for 5 m Piperazine with the Advanced Flash Stripper, in: 3rd Post Combustion Capture Conference and SaskPower Symposium, Saskatchewan, Canada, 2015.